

FLOOD SUSCEPTIBILITY ANALYSIS USING FREELY AVAILABLE DATA, GIS, AND FREQUENCY RATIO MODEL FOR NAGPUR, INDIA

GAURKHEDE, N. T. * – ADANE, V. S.

*Department of Architecture and Planning, Visvesvaraya National Institute of Technology,
Nagpur, Maharashtra 440010, India
(phone: +91-712-222-2828)*

**Corresponding author
e-mail: namrata2707@gmail.com; phone: +91-805-528-2925*

(Received 28th Nov 2022; accepted 7th Apr 2023)

Abstract. Nagpur, the geographical center of India, has witnessed flooding consistently for the past ten years due to urbanization and climate change. Cities like Nagpur, which are newly prone to disasters, need to identify flood-prone areas for planning city development and mitigation measures. Developing countries lack data to generate susceptibility maps, thus remote sensing (RS) and GIS have been used in this study. Ten flood-causing parameters namely altitude, slope, topographic wetness index (TWI), landuse/landcover (LULC), soil texture, rainfall, surface runoff, distance from river, lithology and landforms, have been mapped for Nagpur on ArcGIS10.8 using freely available data. The frequency ratio (FR) model has been adopted, with 70% of flood locations used for machine learning and the remaining 30% for validation. Parameters of surface runoff (FR up to 4.30), landform (FR up to 3.58), lithology (FR up to 2.36), and high rainfall (FR up to 1.82) have shown a maximum positive relationship with the flood-prone areas. The results having 80.90% accuracy and validation of 81.58%. proved that the selected parameters can be robustly adopted for mapping flood susceptible areas.

Keywords: *flood modeling, remote sensing, inland cities, climate change, urban flooding*

Introduction

The International Disaster database of the Centre for Research on the Epidemiology of Disasters (EDMAT, 2019) mapped nine natural disasters around the world from 1970 to 2018 concluding that flood is the most frequently occurring disaster. The flooding scenario is not limited to only coastal cities or cities with higher-order rivers; cities worldwide are threatened by pluvial flooding (Sørensen et al., 2016). According to (Deshkar and Adane, 2016), inland flooding and extreme rainfall events are being witnessed more frequently due to climate change implications. Excessive urbanization has led to rapid changes in the land use of cities, creating more impervious areas thereby increasing runoff and thus overburdening the under-designed drainage system (Gaurkhede et al., 2021).

Mapping flood susceptibility is the starting point in deciphering the areas prone to future floods (Chowdhuri et al., 2020). Owing to a rise in global sea levels, studies and documentation are carried out for coastal flooding (Das, 2020). However, the inland cities witnessing flooding as a combination of urbanization (Pincetl et al., 2013) and climate change (EPA U. S., 2020) also need to be studied. This severity increases with developing countries as they have more population vulnerability and multifaceted social systems (Vasconcelos and Barbassa, 2021).

One of the major challenges in developing countries is the lack of availability of data (Tucci, 2001) to assess the severity of a calamity. For example, the data for natural and

manmade drainage systems useful for planning flood-related infrastructure and resilience building is unavailable in the majority of the developing countries (Tucci, 2001). Various government agencies handle flood disaster management activities in most developing countries (Tingsanchali, 2012). These agencies have different flood mapping systems and methods for the same area, resulting in a lack of insight into the holistic flooding scenario (Tingsanchali, 2012). Flood maps should become an integral part of development plans for these cities. Thus, inland cities in developing countries need to have a simplified, unified and quick methodology for flood mapping, based on easily accessible datasets.

Over the years, several tools and techniques have been used for the identification of flood susceptibility areas. The first and most basic method is a field survey, which is effective but time-consuming and it does not identify the probable future areas prone to flood. Thus, numerous hydraulic models like Storm Water Management Model (SWMM) (Junaidi et al., 2018; Rai et al., 2017), Hydroworks (Bourne, 2020; Bruen and Yang, 2006; Webster et al., 2001), MIKE URBAN (Hossain Anni et al., 2020; Priya, 2019), etc. became popular. However, these are data-intensive (Ahmadisharaf and Daliakopoulos, 2019), require expertise and resources (Osti et al., 2008) which may not be easily available in developing countries (Mahdi El Khalki et al., 2020; Nkwunonwo et al., 2020).

RS has become popular for mapping flooded areas reducing the need for data collection, manpower and expertise (Dewan et al., 2007; Ekeu-wei and Blackburn, 2018). With a combination of LiDAR (Abdullah et al., 2017), Synthetic Aperture Radar data (Wedajo, 2017) and computing systems flood mapping has become a relatively easier task for urban planners. (Abdullah et al., 2017) contends that this airborne data collection is expensive for the already economically weak countries. To demarcate the future flood susceptible areas, a combination of RS, GIS and statistical data models have become popular. Models like Artificial Neural Network (Shafizadehs-Moghadam et al., 2018), Analytical Hierarchical Process (AHP) (Mahmoud and Gan, 2018; Vilasan and Kapse, 2022a), Frequency Ratio (FR), Logistic Regression (LR) and many more are being tested for flood mapping in various scenarios.

FR is a bivariate (Rahmati et al., 2016; Waqas et al., 2021) geospatial assessment tool that calculates the spatial relation of flood parameters to identify flood-prone areas. FR (Natarajan et al., 2021; Samanta et al., 2018; Tehrany et al., 2014) is gaining preference, especially in developing countries due to its simplicity of application. Various methods of flood susceptibility mapping have been compared (Khosravi et al., 2016; Liuzzo et al., 2019) to conclude that the processes based on the statistical indices have the most accurate results, namely the FR model.

Flood events in Nagpur have been increasing in recent years primarily due to two reasons. Firstly, climate change results in increased rainfall intensity (Intergovernmental Panel on Climate Change, 2019), and secondly, urbanization or reduced imperviousness (Avashia and Garg, 2020) leads to flash floods (Dhyani et al., 2018). As per the MoUD of GOI (2015), flooding in the city takes place along most of the man-made drainage system and as per Deshkar (2019) flooding takes place near river channels which are low-lying areas. The situation is critical during the rainy season when wastewater flows into the nearby areas polluting them (MoUD of GOI, 2015). The Disaster Management Cell (DMC) of the NMC is increasingly working towards rescue operations and flood protection walls are being constructed in limited areas near water bodies for protection.

From 1969-2012, the maximum daily rainfall in Nagpur was recorded at 207.1 mm in 1994, which did not lead to any flood events. However, only 144.6 mm and 163 mm of rainfall in 2013 and 2015 respectively, led to flood-like situations (Ansari et al., 2016). The porosity of the ground has been reducing with built-up spaces currently constituting 73% of the city. This altered situation can be attributed to changes in land cover, density and lack of drainage infrastructure.

In almost stark contradiction to this flooding situation; Nagpur historically is also characterized by severe drought situations (Deshkar, 2019), with an alarming regularity, just before monsoon season. This points to the fact that it is in an almost urgent need of an integrated water management system which could or rather should take care of this dichotomy.

Based on this background, this research study has been carried out in Nagpur, an inland city. As a result of the uncontrolled expansion of the city and changing land use, the citizens are witnessing reduced open spaces and thus increased flood events (Lahoti et al., 2019). This clubbed with a change in rainfall patterns has led to several instances of urban flooding in the city (NEERI, 2019).

The objective of the study is to carry out flood susceptibility analysis for Nagpur city through freely and easily available data, using simple spatial analysis model. Flood mapping will help government agencies figure out the reasons for flooding and propose appropriate mitigation strategies (Mahdi El Khalki et al., 2020). It can, and is strongly suggested to, contribute to the holistic design of the city development plan, being done currently.

Material and methods

Study area

Nagpur (21.1458° N, 79.0882° E) is located in the eastern part of the state of Maharashtra (Fig. 1) with an area of 217.56 km^2 . The city is characterized by a high density of population of approximately 11,000 persons per km^2 (Government of India, 2011).

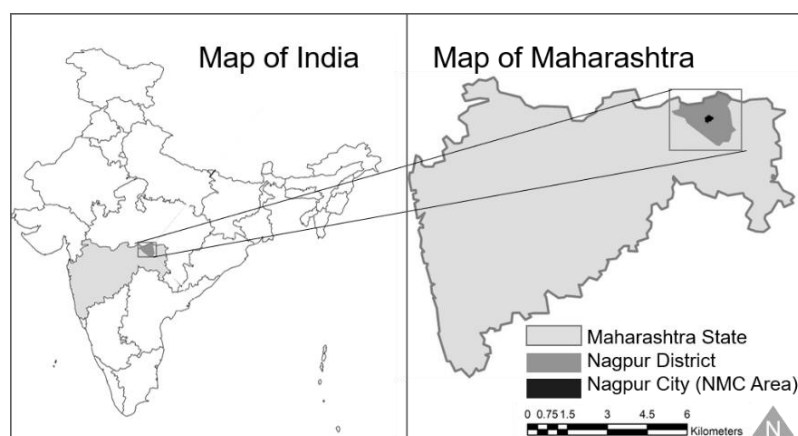


Figure 1. Location of Nagpur city (municipal area)

The Nagpur Municipal Corporation (NMC) area consists of three rivers, Nag in the center, Pili towards the north, and part of the Pora river towards the south. Nagpur has

tropical wet and dry climatic conditions, typically having high-intensity rainfall patterns. Heavy rainfall, with an annual average of 1205 mm can be seen in the southwest monsoon season, June to September (MoUD of GOI, 2015). The temperature ranges from approximately 10 °C to 47 °C throughout the year'. The city falls under the Deccan plateau, having an average elevation of 310 m and has clayey soil in most parts of the city. The city has only 35% of the drainage and sewage infrastructure in place (MoUD of GOI, 2015). Nagpur has started experiencing higher rainfall intensities and yearly flood events over the past decade (NEERI, 2019).

Methodology

The methodology of this research study has been indicated in *Figure 2*.

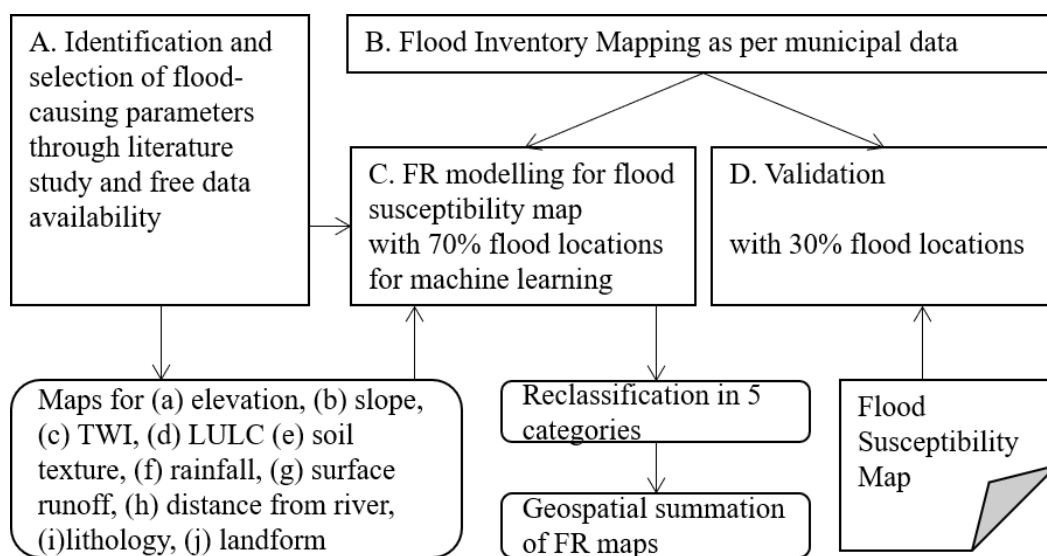


Figure 2. Methodological flowchart for flood susceptibility mapping of Nagpur city

Flood inventory

To predict future flood locations, an inventory of the existing flood-prone areas was prepared. The data on flood locations from 2008 to 2022 was collected from the (DMC-NMC, 2022). 127 submergence points have been identified along eight water channels (Fig. 3).

Flood influencing parameters

Identification of flood-influencing parameters is a critical step in mapping the flood-prone areas. Thirty-four parameters across Science Citation Index research papers were identified and studied in detail to understand the most crucial ones affecting floods. Each study considered seven to fifteen of these parameters. These parameters have been categorized as hydrological, environmental, topographical, and anthropological. Data collection and database preparation for some of the parameters can be tedious and time-consuming, hindering quick decision-making.

Thus, to carry out this study, the parameters were selected on the basis of three criteria: (a) minimum of one parameter from each of the four categories (b) most commonly used in other research studies (c) freely or easily accessible database.

Ten parameters were selected namely; altitude, slope, TWI, LULC, soil texture, rainfall, surface runoff, distance from river, lithology, and landforms. ArcMap 10.8 software (Rezaie et al., 2021; Karabegovi, 2021) was used to prepare geodatabase layers and for final interpolation and validation. *Table 1* details the data collection and *Table 4* provides a summary of the classes of all parameters. All parameters were resampled to bring them to the same spatial resolution of 30 x 30 m grid (Rahman et al., 2021).

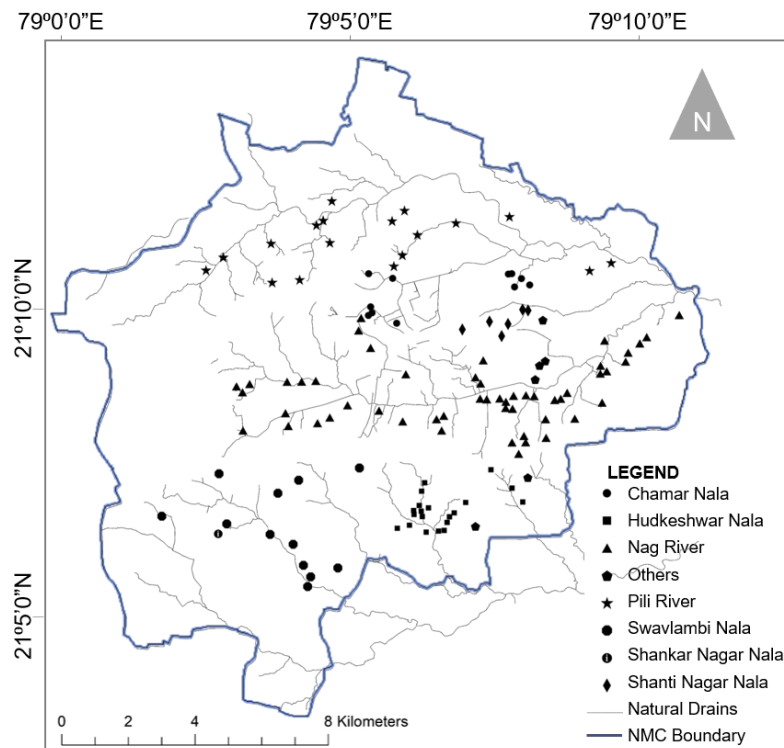


Figure 3. Historical flood locations, 2008-2022, Nagpur city

Table 1. Data collection specifics for selected flood susceptibility parameters

S.N.	Parameter/maps	Unit	Data type	Data source	Year	Resolution
-	Historical flood locations	-	Point	DMC of NMC	2008-2021	-
a	Altitude	m	SRTM DEM Image	USGS	2014	30 m
b	Slope	Degree				
c	TWI	-				
d	LULC	-	Landsat 8 Image	Google Earth	2020	0.3 m
e	Soil texture	-	Raster	FAO, UN	2018	1:50,000
f	Rainfall	mm	NetCDF File Raster	CRU	2009-2020	-
g	Surface runoff	mm	-	-	-	-
h	Distance from river	m	Landsat 8 Image	Google-Earth	2020	0.3 m
i	Lithology	-	Raster	CGWB	2010	-
j	Landforms	-	Raster	Bhuvan Thematic Maps	2005-2006	1:50,000

a. Altitude

The altitude of an area is related to its distance from sea level and its climatic condition (Rahmati et al., 2016; Shafizadeh-Moghadam et al., 2018). It can also affect

vegetation growth and other topographic factors (Janizadeh et al., 2019; Nachappa et al., 2020). The elevation map for Nagpur was prepared through the spatial analysis tool in ArcGIS 10.8 using freely available Shuttle Radar Topography Mission (SRTM) Digital Elevation Model (DEM) 2014, from the United States Geological Survey (USGS). Altitude has been categorized into nine classes (*Fig. 4a*), ranging from 280 m to 370 m, with the lowest elevation intuitively having the highest possibility of getting flooded.

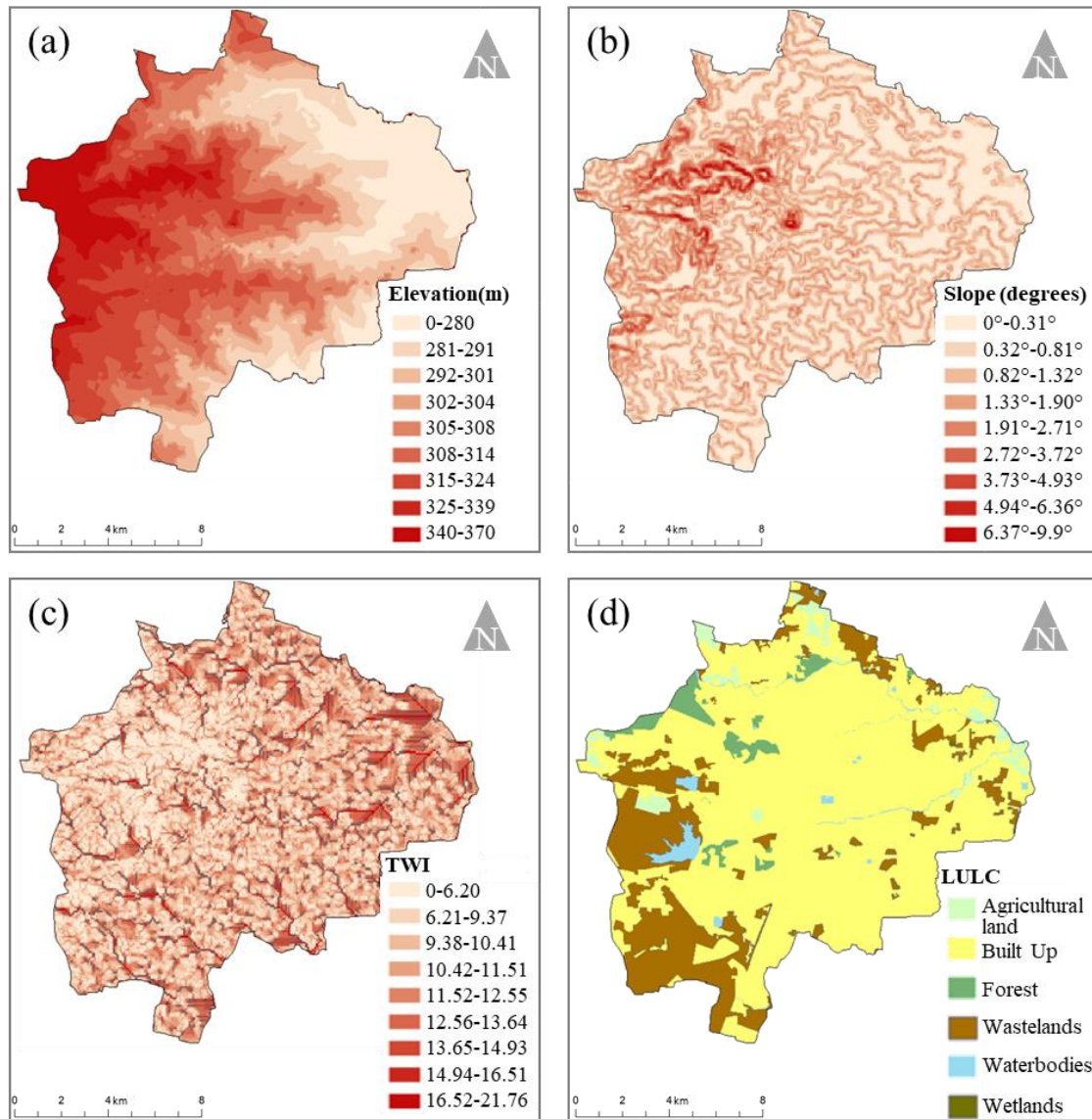


Figure 4. Parameters used for FR modelling: (a) altitude, (b) slope, (c) TWI, (d) LULC

b. Slope

The degree of the slope controls the runoff, demarcating zones of submergence of areas or its water retention capability (Das and Gupta, 2021; Waqas et al., 2021). It also affects the runoff velocity (Rincón et al., 2018; Shafizadeh-Moghadam et al., 2018) and the vertical percolation of rainfall (Samanta et al., 2018). Thus, it forms a part of all

flood susceptibility studies and simulations. The slope map of Nagpur was also prepared through a spatial analysis tool in ArcGIS with SRTM DEM 2014 data. It was categorized into nine classes (*Fig. 4b*), from 0.31° to 9.9° with the maximum slope having the lowest flood vulnerability.

c. Topographic wetness index

The TWI, a function of the topography of an area indicates the spatial distribution of its wetness conditions (Bui et al., 2020; Termeh et al., 2018). The TWI map for Nagpur (*Fig. 4c*) was prepared on ArcGIS with SRTM DEM as the input and calculated using Equation 1:

$$TWI = Ln\left(\frac{a}{\tan B}\right) \quad (\text{Eq.1})$$

where *Catchment Area*, $a = \frac{\text{Total area}}{\text{Length of the contour}}$ and $B = \text{Slope in degrees}$.

It was categorized into nine classes from a value < 6.20 to as high as 21.76. Higher TWI indicates a higher flood probability in an area (Nsangou et al., 2022; Swain et al., 2020), only around 8% of the city has high TWI.

d. Land use/land cover

LULC directly or indirectly indicates permeability (Vilasan and Kapse, 2022b) and runoff (Andaryani et al., 2021; Hammami et al., 2019; Nsangou et al., 2022) due to the properties of surface finish materials (Kaur et al., 2017). Areas with more built-up have a higher probability of getting flooded and more devastation than green areas (Liuzzo et al., 2019; Pham et al., 2020). The map of LULC was prepared through the visual interpretation of freely available Google Earth Satellite Image 2020. Six LULC categories (*Fig. 4d*) were considered as per classes defined by (NRSC, 2014). In Nagpur, the built-up has increased from 59% to 74% (as per satellite imagery) in the last decade.

e. Soil texture

Soil quality decides the infiltration capabilities of any soft surface (Kaur et al., 2017; Waqas et al., 2021). Soil with more porosity will lead to reduced flood hazards (Swain et al., 2020). The soil map was generated using the Food and Agriculture Organization (FAO) Soils Portal of the United Nations (UN). Nagpur has 91.5% of clayey and 8.47% of clay soils (*Fig. 5e*), categorized as Group D soils by the United States Department of Agriculture, which have moderate to low infiltration characteristics.

f. Rainfall

Rainfall is one of the most crucial parameters for flood susceptibility mapping (Rincón et al., 2018), especially with climate change scenarios leading to intense rainfall patterns. Nagpur city gets an annual average rainfall of 1205 mm (DDMA Nagpur, 2018) and 90% of its rainfall is concentrated in four months of the year (MoUD of GOI, 2015), creating an extreme situation in the city. Most researchers (Rincón et al., 2018; Tang et al., 2018; Yariyan et al., 2020) have considered rainfall as a flood causing parameter, although the exact amount of rainfall that will lead to a flood cannot be

determined on a standalone basis (Das and Gupta, 2021). Average annual rainfall for ten years, 2011-2020 was considered and Inverse Distance Weighting (IDW) interpolation method was adopted to map the data. The rainfall data was downloaded as NetCDF File Raster Layer from Climate Research Unit (CRU), which is freely available data. The city is divided into eight rainfall zones with minor variations in ranges (*Fig. 5f*).

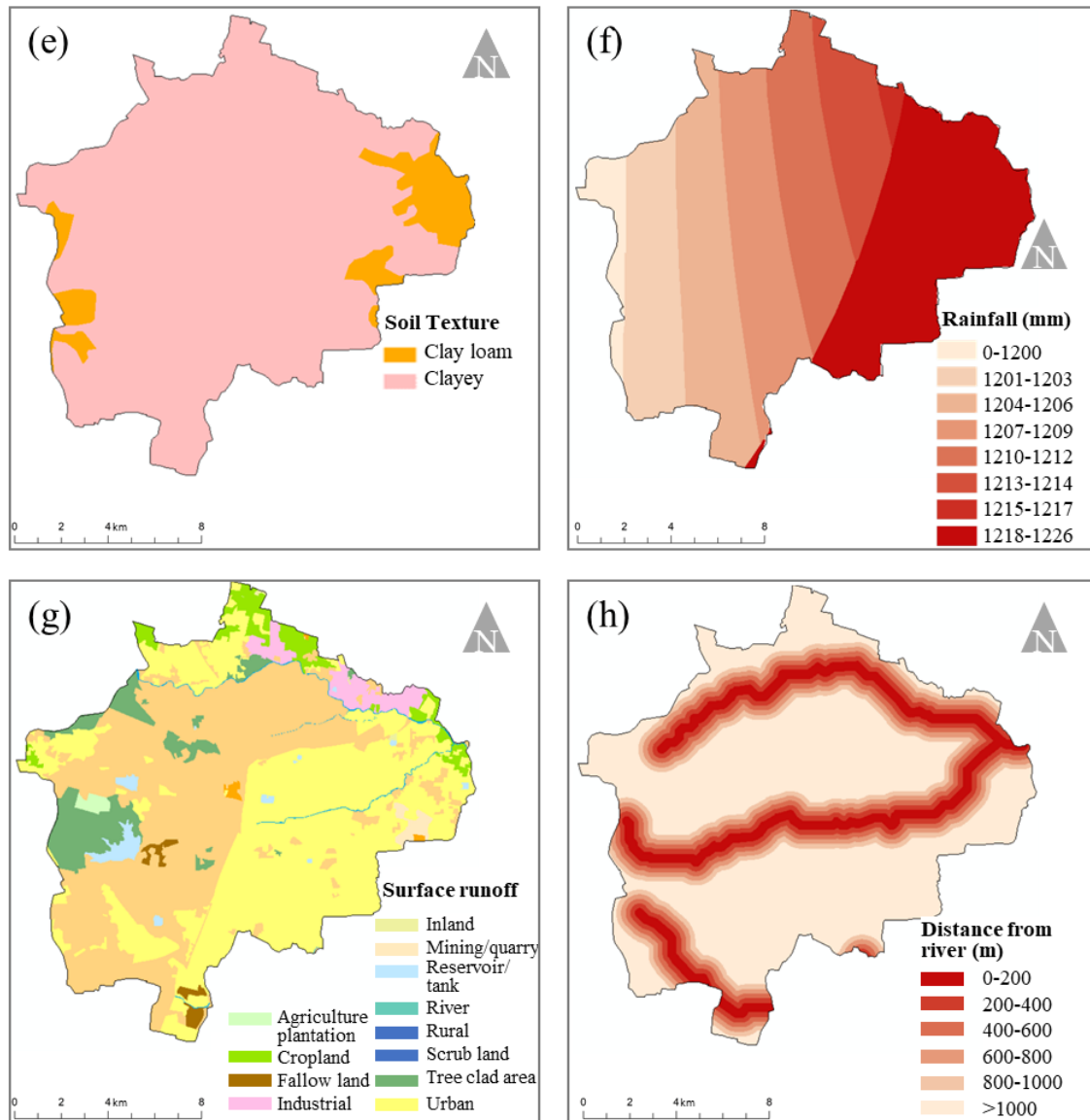


Figure 5. Parameters used for FR modelling: (e) soil texture, (f) rainfall, (g) surface runoff, (h) distance from river

g. Surface runoff

Surface runoff is one of the most significant criterion to identify flood zones in urban areas, due to the lack of infiltration areas (Pal and Samanta, 2011). Curve Number (CN), a permeability factor, is an indicator of the surface runoff capability of a particular LULC area (Vojtek and Vojteková, 2019). In this study Soil Conservation

Service (SCS) method (Symeonakis and Drake, 2010) was used to calculate the runoff quantity, Q in millimeters (as shown in Eq. 2):

$$Q = \frac{(P - Ia)^2}{P - Ia + S} \quad (\text{Eq.2})$$

where:

P = storm rainfall event,

S = potential maximum retention in millimeters = $\left(\frac{25400}{CN}\right) - 254$,

Ia = Initial abstraction in millimeters = $0.2S$.

The curve numbers for the co-relation of LULC and soil group were adopted from Halley et al. (2000) represented in Table 2. According to the NMC, the storm rainfall event in July 2013 caused maximum damage in terms of life and property in the city. Thus, the maximum rainfall for five consecutive days in July 2013, 333.33 mm (Indian Meteorological Department), was considered as the storm rainfall data. This data map was prepared based on other freely available parameters (Fig. 5f).

Table 2. Runoff calculation for each land use/land cover area

LULC	Soil group	CN	Area		S	Ia	P (mm)	Q (mm)
			Ha	%				
Agricultural land	D	87	1131	5.35%	37.95	7.59	333.33	291.75
Built-up	D	87	15666	74.16%	37.95	7.59	333.33	291.75
Forest	D	77	1355	6.41%	75.87	15.17	333.33	256.89
Wastelands	D	78	2578	12.21%	71.64	14.32	333.33	260.50
Water bodies	D	98	391	1.85%	5.18	1.03	333.33	327.19
Wetlands	D	90	5	0.03%	28.22	5.64	333.33	301.70

h. Distance from river

Proximity to rivers has been seen as a significant parameter for flood susceptibility (Khosravi et al., 2016), as rivers naturally are the points of the congregation for rainfall-runoff (Yariyan et al., 2020). Chronic flood-prone areas are usually located near water bodies (Swain et al., 2020) as the water overflows to the nearest water body (Wang et al., 2019). A map of water bodies was prepared using ArcGIS tools with DEM as the base map. Use of ArcGIS tools namely; fill sinks, followed by flow accumulation, and Strahler order (Steiner and Grillmair, 1973) led to the final map of water bodies. The highest order streams (3 nos.) were selected and their buffer map was prepared using the Euclidean distance (Chen et al., 2017) in ArcGIS. The study area was thus divided into six categories (Fig. 5h) namely, 0-200 m, 200-400 m, 400-600 m, 600-800 m, 800-1000 m and > 1000 m.

i. Lithology

Lithology governs the permeability of a land parcel, spatial and temporal variations of drainage basins (Andaryani et al., 2021; Vojtek and Vojteková, 2019) and it indicates the land's erodibility (Rahmati et al., 2016). Thus, it affects the runoff generation (Costache et al., 2020a; Janizadeh et al., 2019). A lithology map of Nagpur was

prepared using freely available data from the Central Ground Water Board of India (CGWB, 2016), categorized into five classes (*Fig. 6i*). The characteristics and distribution of lithology is explained in *Table 3*.

Table 3. Distribution of lithology in the NMC area

Type	Geological age	Area		Depth (m)	Features	In-filtration
		Ha	%			
Alluvium	Recent subrecent	45	2.19	25-35	Medium to coarse-grained sand with/without clay	Poor
Archeans	Archeans	491	23.69	20-25	Weathered zone forms a shallow aquifer. Un-weathered crystalline rocks have an occurrence of groundwater through joints/fractures	Moderate
Deccan Trap (Basalt)	Upper cretaceous to lower Eocene	1194	57.61	15-30	Intertapean clay deposits are found between two of these layers. Groundwater is present in pores, joints and fractures	Good
Gondwana	Lower to upper Permian	2013	9.71	45-50	Constantly water-saturated due to water-bearing formations	Very poor
Lameta	Upper carboniferous to lower cretaceous	1409	6.80	15-20	Compact and clayey	Poor

j. Landform

Landform, indicating land permeability varies as per type of rocks, affecting the absorption and thus overland flow of inundation (Rahman et al., 2019; Samanta et al., 2018). The landform map was prepared with the freely available thematic map of geomorphology on the Bhuvan Portal of NRSC, 2005-06. It comes in five categories in the city (*Fig. 6j*). Most of the city areas are covered with pediplains. Pediplains are formed through erosion and may or may not have thin cover of debris.

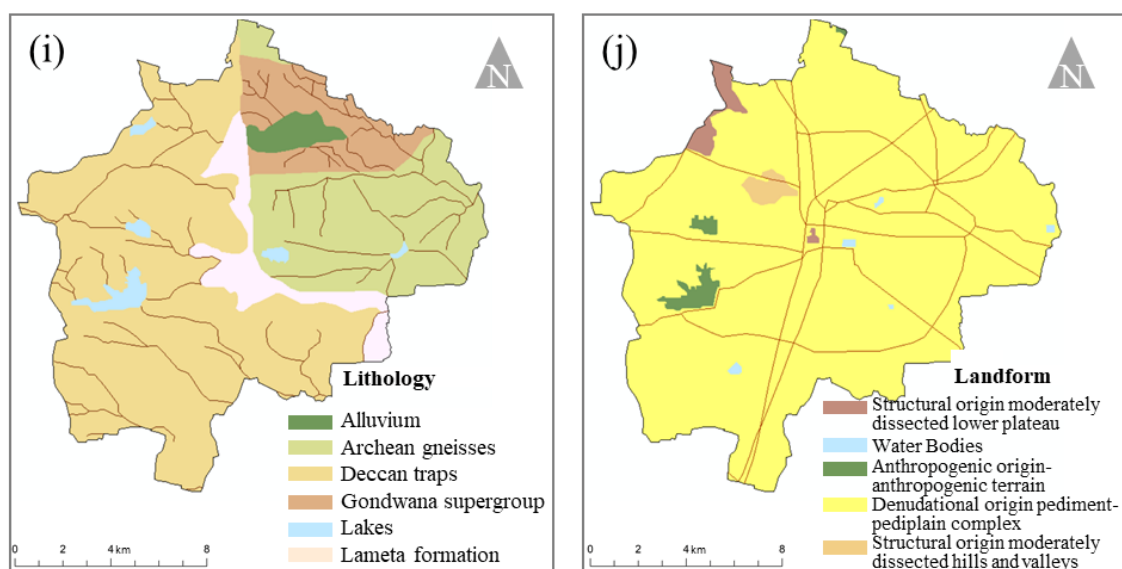


Figure 6. Parameters used for FR modelling: (i) lithology, (j) landform

Model for mapping of susceptible locations

From the plethora of models available, the frequency ratio model, a bivariate method was selected. (Natarajan et al., 2021; Pham et al., 2020; Samanta et al., 2018; Rahmati et al., 2016; Tehrany et al., 2014) have used this model, which spatially relates the flood location to each flood parameter. It is one of the simplest statistical methods, which works on the GIS platform and does not require any other specialized software or expertise to carry out the modelling.

In this study, 70% (Costache et al., 2020b; Janizadeh et al., 2019; Wang et al., 2019), 89 out of 127 of historical flood locations, selected randomly were used for machine-learning. FR for each category of a parameter is a proportion of the flooded area in the total study area, calculated using *Equation 3*:

$$FR = \frac{\frac{E}{F}}{\frac{M}{L}} \quad (\text{Eq.3})$$

where E = number of flood locations; F = total number of flood locations; M = area covered by each parameter; L = total study area (Jaafari et al., 2014; Regmi et al., 2014).

The FR in raster images of each parameter were reclassified into five category ranges of very high, high, moderate, low and very low to carry out geospatial summation in ArcGIS. This overlap resulted in the Flood Susceptibility Index (FSI) map of the area, calculated using *Equation 4*:

$$FSI = \sum FR \quad (\text{Eq.4})$$

Results, validation, and discussion

The higher the FR (*Table 4*), the higher is the connection of the flood-causing parameter to the flood-susceptible areas.

Lower altitudes of classes 281-291, 292-301, 302-304 and 305-308 show high co-relation to flood locations with FR of 1.12, 1.57, 1.35 and 1.08 respectively. Slope ranges of 0.82°-1.32° and 1.33°-1.90° (constituting in all 40.48% of the total area) have a FR of more than 1.1, indicating that these slopes have higher flood possibility. TWI 11.52-12.55 has a maximum FR of 1.16, indicating moderate relationship with flood prone areas.

In the LULC parameter, the built-up area has a high FR of 1.24 and water bodies have a FR of 1.2. Thus, low permeability in the built-up area indicates a high probability of getting flooded. Soil textures of both classes present in Nagpur have a FR close to 1, indicating moderate co-relation of soil to flood zones. The rainfall range of 1218-1226 mm covers an area of 27.23% and has a high FR of 1.82. Surface runoff which is a function of land use, soil and rainfall has the highest FR of 4.30 for rural land use in Nagpur city. Concurrently, urban and reservoir/tank areas have a high FR value of 1.41 and 1.71 respectively. Thus, surface runoff shows a very high positive co-relation to flood susceptibility of an area, indicating it to be a parameter which majorly governs frequency of an area being flooded.

Distance from river in case of Nagpur shows that only 37 flood points out of 89 are located up to a distance of 1000 m from the river. This parameter may show better results if the next order of rivers is considered. The maximum FR for distance from river can be

noted as 1.16 for the 800-1000 m distance from river. In lithology, the Deccan Traps which cover 56.53% of the city has a FR of only 0.71 and Lameta Formation has the highest FR of 2.18, making Lameta a more probable zone for flooding. The landform of Nagpur is 95.95% Denudational Origin Pediment- Pediplain Complex, having a FR of 1.03 and the water bodies understandably show a very high FR of 3.58.

Table 4. Frequency ratios of flood-causing parameters for flood susceptibility mapping

S. N.	Parameter	Range	Area		Flood points	FR
			Ha	%		
a	Altitude	0-280	2759	13.06	10	0.66
		281-291	2691	12.74	17	1.12
		292-301	2761	13.07	20	1.57
		302-304	743	3.52	5	1.35
		305-308	2799	13.25	14	1.08
		308-314	2771	13.12	12	0.87
		315-324	3248	15.37	9	0.60
		325-339	1782	8.43	2	0.21
		340-370	1553	7.35	0	0.00
b	Slope	0°-0.31°	6597	31.23	28	1.01
		0.32°-0.81°	4356	20.62	18	0.98
		0.82°-1.32°	4918	23.28	24	1.16
		1.33°-1.90°	3633	17.20	17	1.11
		1.91°-2.71°	793	3.76	0	0.00
		2.72°-3.72°	422	2.00	1	0.56
		3.73°-4.93°	229	1.08	1	1.04
		4.94°-6.36°	106	0.50	0	0.00
		6.37°-9.9°	39	0.19	0	0.00
c	TWI	0-6.20	3215	15.22	14	1.03
		6.21-9.37	5054	23.93	22	1.03
		9.38-10.41	4189	19.83	19	1.08
		10.42-11.51	3163	14.97	13	0.98
		11.52-12.55	2043	9.67	10	1.16
		12.56-13.64	1643	7.78	6	0.87
		13.65-14.93	1005	4.76	2	0.47
		14.94-16.51	559	2.65	2	0.85
		16.52-21.76	237	1.12	1	1.00
d	LULC	Agricultural land	1016	4.81	1	0.23
		Built up	15666	74.16	82	1.24
		Forest	1355	6.41	0	0.00
		Wastelands	2678	12.68	4	0.35
		Water bodies	397	1.88	2	1.20
		Wetlands	14	0.07	0	0.00
e	Soil texture	Clay loam	1790	8.47	8	1.06
		Clayey	19335	91.53	81	1.00
f	Rainfall	< 1200	709	3.35	0	0
		1201-1203	2753	13.03	1	0.09
		1204-1206	3655	17.30	9	0.58
		1207-1209	3285	15.55	13	0.94
		1210-1212	2937	13.90	18	1.45
		1213-1214	1853	8.77	3	0.38
		1215-1217	182	0.86	1	1.31
		1218-1226	5752	27.23	44	1.82

S. N.	Parameter	Range	Area		Flood points	FR
			Ha	%		
g	Surface runoff	Cropland	756	3.58	1	0.31
		Fallow land	167	0.79	0	0.00
		Agriculture plantation	93	0.44	0	0.00
		Urban	8744	41.39	52	1.41
		Rural	55	0.26	1	4.30
		Industrial	584	2.76	0	0.00
		Mining/quarry	146	0.69	0	0.00
		Tree clad area	1355	6.41	0	0.00
		Scrub land	8814	41.72	33	0.89
		Reservoir/tank	278	1.31	2	1.71
		River	115	0.54	0	0.00
		Inland	18	0.09	0	0.00
h	Distance from river	0-200	1871	8.86	7	0.89
		200-400	1867	8.84	9	1.14
		400-600	1853	8.77	6	0.77
		600-800	1851	8.76	6	0.77
		800-1000	1835	8.68	9	1.16
		> 1000	11848	56.09	52	1.04
i	Lithology	Alluvium	453	2.14	3	1.57
		Archean gneisses	4911	23.25	37	1.79
		Deccan traps	11941	56.53	32	0.64
		Gondwana supergroup	2013	9.53	3	0.35
		Lakes	398	1.89	0	0.00
		Lameta formation	1409	6.67	14	2.36
j	Landform	Structural origin moderately dissected lower plateau	296	1.40	0	0.00
		Water bodies	66	0.31	1	3.58
		Anthropogenic origin-anthropogenic terrain	288	1.36	0	0.00
		Denudational origin pediment- pediplain complex	20270	95.95	88	1.03
		Structural origin moderately dissected hills and valleys	205	0.97	0	0.00

Geospatial summation of ten FR maps for the 89 flood locations used for machine-learning, led to the preparation of the final flood susceptibility map (*Fig. 7*). The success rate of the method is calculated based on the sum of the percentages of very high and high susceptibility classes, as indicated in *Table 5* which has an accuracy result of 80.90%. There are many models to assess flood susceptibility but it is important to validate it. Thus, the remaining 30% (Nohani et al., 2019), 38 out of 127, historic flood locations were taken for validating the final susceptibility map. It indicated a high prediction accuracy of 81.58% (*Table 5*). The very high and high flood susceptibility zones with an FSI of 10.3-11.78 and 11.79-15.80 which constitutes 48.13%) of the study area. This is a very high proportion of the city area, considering the fact that Nagpur was historically regraded as a city well buffered and safe from disasters (*Table 6*).

Table 5. Prediction accuracy and success rate for the flood susceptibility analysis

S. N.	Flood susceptibility class	Training (89 flood locations)	Success rate (high to very high)	Validation (38 flood locations)	Prediction accuracy (high to very high)
1	Very high	47	80.90%	22	81.58%
2	High	25		9	
3	Moderate	15		5	
4	Low	2		1	
5	Very low	0		1	

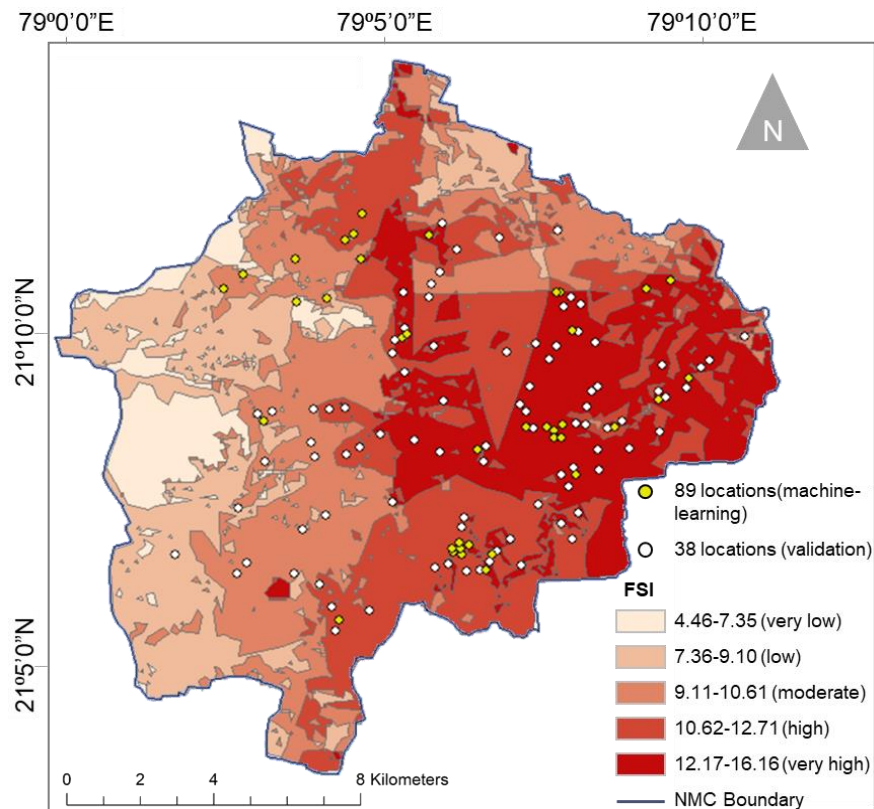


Figure 7. FR model-based flood susceptibility index with historical flood locations

Table 6. Flood susceptibility areas, Nagpur

S. N.	Flood susceptibility class	Area under flood vulnerability	
		ha	%
1	Very high	4743	22.46
2	High	5443	25.77
3	Moderate	5536	26.21
4	Low	3986	18.87
5	Very low	1413	6.69

The overall prediction accuracy of 81.58% can be increased by 5-6% if only selected 7-8 parameters are considered. The parameters, distance from river, soil texture and TWI, showing low FR can be excluded from the FR summation to achieve better results. The results of the study show that considering soil texture and TWI parameters in a highly urbanized area has shown weak to moderate relation to the FR. This is on account of the impervious nature of the surface in urban areas. Another iteration of this was conducted replacing rainfall with soil drainage, which resulted in 93% accuracy of the model. It was not used in the final study as getting soil drainage data may not be a simple task for urban planners. The Frequency Ratio Model thus can be very effective in demarcating flood susceptible zones, with selection of appropriate parameters. A combination of other models like the LR, ANN, or others with the Frequency Ratio spatial analysis may provide better results than the current study.

A limitation of the current study is the lack of ground verification of the data provided by the urban local body, which has been considered as the base and most crucial data for the study.

The flood susceptibility map generated from such studies can provide urban local bodies with the actual flood risk zones, rather than just flood spots. A lot of developing countries that lack sewage and drainage infrastructure to handle flood situations can adopt this methodology to demarcate high risk zones. This can help calculate and design the capacity of infrastructure systems better. The study can be taken as a base to plan for Sustainable Urban Drainage Systems (SuDS), enhancing the natural drainage system instead of the piped ones. It can include identification and enhancement of pervious areas in the city. SuDS, in these highly vulnerable areas, can reduce the extent and impact of floods at this early stage of risk.

Conclusion

The current research has used the FR model for demarcating and analyzing flood susceptibility zones in Nagpur city. The availability of data in developing countries is seen as a deterring factor to carry out disaster mapping of cities (Ghansah et al., 2021). Thus, emphasis on open-source data, to support the urban local bodies in relation to the otherwise tedious task of mapping was the most important factor in the selection of parameters for this study. A geospatial database was used to prepare maps for ten parameters namely; elevation, slope, TWI, LULC, soil texture, rainfall, surface runoff, distance from river, lithology and landforms. The study used 89 out of 127 historical flood locations in Nagpur selected randomly for the FR model, and the remaining 38 were used for validation of the results.

The parameters of surface runoff (FR up to 4.30), landform (FR up to 3.58), lithology (FR up to 2.36) and rainfall (FR up to 1.82) have shown a very strong positive relation with the historical flood locations. The parameters of LULC (FR up to 1.24), elevation (FR up to 1.57), slope (FR up to 1.16), distance from river (FR up to 1.16), TWI (FR up to 1.16) and soil texture (FR up to 1.05) show a moderately positive relationship to the flood susceptible areas. Thus, the selection of parameters for the Nagpur city is appropriate. It is important to note that the parameters of TWI and soil texture may show a stronger relationship with the flood-prone locations in cities with more open spaces and less built-up density.

Therefore, the FR model with an accuracy of 81.58% with the selected parameters proves to be an effective method for quick mapping of flood-prone locations in any city. The land parcels demarcated in *Figure 7* with very high and high susceptibility index have the highest probability of getting flooded.

This methodology and model can be used by government agencies and research institutions, which traditionally lack a database, for identifying flood-prone zones while undertaking land use and infrastructure planning. Subsequently; this methodology and model can also be purposed to resolve the dichotomy of, earlier mentioned, pre-monsoon droughts followed by monsoon floods through the application of a retention detention approach and timing it quite efficiently to tide over this problem. FR model uses the GIS platform and does not require any additional expertise. Thus, this methodology can be tested in other Indian cities and other developing countries for further validation, especially the selection of parameters.

REFERENCES

- [1] Abdullah, A. F., Vojinovic, Z., Meesuk, V. (2017): Modeling Flood Disasters: Issues Concerning Data for 2D Numerical Models. – MATEC Web of Conferences 103. <https://doi.org/10.1051/mateconf/201710304008>.
- [2] Ahmadisharaf, E., Daliakopoulos, I. N. (2019): 14. Artificial Neural Networks for Flood Susceptibility Mapping in Data-Scarce Urban Areas. – In: Pourghasemi, H. R. et al. (eds.) Spatial Modeling in GIS and R for Earth and Environmental Sciences. Elsevier, Amsterdam, pp. 323-336. <https://doi.org/10.1016/B978-0-12-815226-3.00014-4>.
- [3] Andaryani, S., Nourani, V., Haghighi, A. T., Keesstra, S. (2021): Integration of hard and soft supervised machine learning for flood susceptibility mapping. – Journal of Environmental Management 291(November 2020): 112731. <https://doi.org/10.1016/j.jenvman.2021.112731>.
- [4] Ansari, T. A., Katpatal, Y. B., Vasudeo, A. D. (2016): Spatial evaluation of impacts of increase in impervious surface area on SCS-CN and runoff in Nagpur urban watersheds, India. – Arabian Journal of Geosciences 9(18). <https://doi.org/10.1007/s12517-016-2702-5>.
- [5] Avashia, V., Garg, A. (2020): Implications of land use transitions and climate change on local flooding in urban areas: an assessment of 42 Indian cities. – Land Use Policy 95(February): 104571. <https://doi.org/10.1016/j.landusepol.2020.104571>.
- [6] Bourne, L. (2020): Implementation Guidelines. – In: Stakeholder Relationship Management. Routledge, London, pp. 193-220. <https://doi.org/10.4324/9781315610573>.
- [7] Bruen, M., Yang, J. (2006): Combined hydraulic and black-box models for flood forecasting in urban drainage systems. – Journal of Hydrologic Engineering 11(6): 589-596. [https://doi.org/10.1061/\(asce\)1084-0699\(2006\)11:6\(589\)](https://doi.org/10.1061/(asce)1084-0699(2006)11:6(589)).
- [8] Bui, Q. T., Nguyen, Q. H., Nguyen, X. L., Pham, V. D., Nguyen, H. D., Pham, V. M. (2020): Verification of novel integrations of swarm intelligence algorithms into deep learning neural network for flood susceptibility mapping. – Journal of Hydrology 581: 124379. <https://doi.org/10.1016/j.jhydrol.2019.124379>.
- [9] CGWB (2016): Aquifer Maps and Ground Water Management Plan (Issue March). – [http://cgwb.gov.in/AQM/NAQUIM_REPORT/Maharashtra/Bhokardan Taluka, Jalna District, \(Part-I\).pdf](http://cgwb.gov.in/AQM/NAQUIM_REPORT/Maharashtra/Bhokardan Taluka, Jalna District, (Part-I).pdf).
- [10] Chen, W., Pourghasemi, H. R., Zhao, Z. (2017): A GIS-based comparative study of Dempster-Shafer, logistic regression and artificial neural network models for landslide susceptibility mapping. – Geocarto International 32(4): 367-385. <https://doi.org/10.1080/10106049.2016.1140824>.
- [11] Chowdhuri, I., Pal, S. C., Chakraborty, R. (2020): Flood susceptibility mapping by ensemble evidential belief function and binomial logistic regression model on river basin of eastern India. – Advances in Space Research 65(5): 1466-1489. <https://doi.org/10.1016/j.asr.2019.12.003>.
- [12] Costache, R., Pham, Q. B., Sharifi, E., Linh, N. T. T., Abba, S. I., Vojtek, M., Vojteková, J., Nhi, P. T. T., Khoi, D. N. (2020a): Flash-flood susceptibility assessment using multi-criteria decision making and machine learning supported by remote sensing and GIS techniques. – Remote Sensing 12(1). <https://doi.org/10.3390/RS12010106>.
- [13] Costache, R., Țincu, R., Elkhachy, I., Pham, Q. B., Popa, M. C., Diaconu, D. C., Avand, M., Costache, I., Arabameri, A., Bui, D. T. (2020b): New neural fuzzy-based machine learning ensemble for enhancing the prediction accuracy of flood susceptibility mapping. – Hydrological Sciences Journal 65(16): 2816-2837. <https://doi.org/10.1080/02626667.2020.1842412>.
- [14] Das, S. (2020): Flood susceptibility mapping of the Western Ghat coastal belt using multi-source geospatial data and analytical hierarchy process (AHP). – Remote Sensing Applications: Society and Environment 20(August): 100379. <https://doi.org/10.1016/j.rsase.2020.100379>.

- [15] Das, S., Gupta, A. (2021): Multi-criteria decision based geospatial mapping of flood susceptibility and temporal hydro-geomorphic changes in the Subarnarekha basin, India. – *Geoscience Frontiers* 12(5): 101206. <https://doi.org/10.1016/j.gsf.2021.101206>.
- [16] DDMA Nagpur (2018): District Disaster Management Plan Nagpur District. – <https://static.s3waas.gov.in/s3d1f491a404d6854880943e5c3cd9ca25/uploads/2018/03/2018031651.pdf>.
- [17] Deshkar, S. (2019): Resilience Perspective for Planning Urban Water Infrastructures: A Case of Nagpur City. – In: Ray, B., Shaw, R. (eds.) *Urban Drought. Disaster Risk Reduction*. Springer, Singapore. https://doi.org/10.1007/978-981-10-8947-3_9.
- [18] Deshkar, S., Adane, V. (2016): Community resilience approach for prioritizing infrastructure development in urban areas. – *Urban Disasters and Resilience in Asia* 2018(April): 245-267. <https://doi.org/10.1016/B978-0-12-802169-9.00016-1>.
- [19] Dewan, A. M., Islam, M. M., Kumamoto, T., Nishigaki, M. (2007): Evaluating flood hazard for land-use planning in greater Dhaka of Bangladesh using remote sensing and GIS techniques. – *Water Resources Management* 21(9): 1601-1612. <https://doi.org/10.1007/s11269-006-9116-1>.
- [20] Dhyani, S., Lahoti, S., Khare, S., Pujari, P., Verma, P. (2018): Ecosystem based Disaster Risk Reduction approaches (EbDRR) as a prerequisite for inclusive urban transformation of Nagpur City, India. – *International Journal of Disaster Risk Reduction* 32(November 2017): 95-105. <https://doi.org/10.1016/j.ijdr.2018.01.018>.
- [21] DMC-NMC (2022): Disaster Management Plan 2022-23. – Nagpur Municipal Corporation. https://www.nmcnagpur.gov.in/assets/250/2022/07/mediafiles/Aapatti_Vyavsthan_Ara khada2022.pdf.
- [22] EDMAT (2019): OFDA/CRED International Disaster Database. – Université Catholique de Louvain, Brussels.
- [23] Ekeu-wei, I. T., Blackburn, G. A. (2018): Applications of open-access remotely sensed data for flood modelling and mapping in developing regions. – *Hydrology* 5(3). <https://doi.org/10.3390/hydrology5030039>.
- [24] EPA U. S. (2020): Climate change and social vulnerability in the United States: a focus on six impacts. – National Centers for Environmental Information. <https://doi.org/10.25921/STKW-7W73>.
- [25] Gaurkhede, N., Adane, V. S., Khonde, S. (2021): Identification of interruptions in urban drainage systems and their sustainable solutions for alleviating flood risk in Mumbai, an Indian megacity. – *Journal of Integrated Disaster Risk Management* 11(1): 108-130. <https://doi.org/10.5595/001c.30705>.
- [26] Ghansah, B., Nyamekye, C., Owusu, S. (2021): Mapping flood prone and Hazards Areas in rural landscape using LANDSAT images and random forest classification: case study of Nasia watershed in Ghana. – *Cogent Engineering* 8(1). <https://doi.org/10.1080/23311916.2021.1923384>.
- [27] Government of India (2011): Census of India 2011. – <https://www.census2011.co.in/census/city/353-nagpur.html>.
- [28] Halley, M. C., White, S. O., Watkins, E. W. (2000): ArcView GIS Extension for Estimating Curve Numbers. – <https://proceedings.esri.com/library/userconf/proc00/professional/papers/PAP657/p657.htm>.
- [29] Hammami, S., Zouhri, L., Souissi, D., Souei, A., Zghibi, A., Marzougui, A., Dlala, M. (2019): Application of the GIS based multi-criteria decision analysis and analytical hierarchy process (AHP) in the flood susceptibility mapping (Tunisia). – *Arabian Journal of Geosciences* 12(21). <https://doi.org/10.1007/s12517-019-4754-9>.
- [30] Hossain Anni, A., Cohen, S., Praskievicz, S. (2020): Sensitivity of urban flood simulations to stormwater infrastructure and soil infiltration. – *Journal of Hydrology* 588(April). <https://doi.org/10.1016/j.jhydrol.2020.125028>.

- [31] Intergovernmental Panel on Climate Change (2019): Global Warming of 1.5 °C. – In Special Report on Global Warming of 1.5 °C. IPCC, Geneva.
- [32] Jaafari, A., Najafi, A., Pourghasemi, H. R., Rezaeian, J., Sattarian, A. (2014): GIS-based frequency ratio and index of entropy models for landslide susceptibility assessment in the Caspian for ... Related papers. – International Journal of Environmental Science and Technology. <https://doi.org/10.1007/s13762-013-0464-0>.
- [33] Janizadeh, S., Avand, M., Jaafari, A., Phong, T. V. (2019): Prediction success of machine learning methods for flash flood susceptibility mapping in the Tafresh Watershed, Iran. – Sustainability 11(19): 5426. <https://doi.org/10.3390/su11195426>.
- [34] Junaidi, L. M., Ermalizar, L. M., Junaidi, A. (2018): Flood simulation using EPA SWMM 5.1 on small catchment urban drainage system. – MATEC Web of Conferences 229: 1-9. <https://doi.org/10.1051/mateconf/201822904022>.
- [35] Karabegovi, I. (2021): Lecture notes in networks and systems new technologies, development and application IV. – https://doi.org/https://doi.org/10.1007/978-3-030-75275-0_84.
- [36] Kaur, H., Gupta, S., Parkash, S., Thapa, R., Mandal, R. (2017): Geospatial modelling of flood susceptibility pattern in a subtropical area of West Bengal, India. – Environmental Earth Sciences 76(9). <https://doi.org/10.1007/s12665-017-6667-9>.
- [37] Khosravi, K., Nohani, E., Maroufinia, E., Pourghasemi, H. R. (2016): A GIS-based flood susceptibility assessment and its mapping in Iran: a comparison between frequency ratio and weights-of-evidence bivariate statistical models with multi-criteria decision-making technique. – Natural Hazards 83(2): 947-987. <https://doi.org/10.1007/s11069-016-2357-2>.
- [38] Lahoti, S., Kefi, M., Lahoti, A., Saito, O. (2019): Mapping methodology of public urban green spaces using GIS: an example of Nagpur City, India. – Sustainability (Switzerland) 11(7): 1-23. <https://doi.org/10.3390/su10022166>.
- [39] Liuzzo, L., Sammartano, V., Freni, G. (2019): Comparison between different distributed methods for flood susceptibility mapping. – Water Resources Management 33(9): 3155-3173. <https://doi.org/10.1007/s11269-019-02293-w>.
- [40] Mahdi El Khalki, E., Trambly, Y., Massari, C., Brocca, L., Simonneaux, V., Gascoin, S., El Mehdi Saidi, M. (2020): Challenges in flood modeling over data-scarce regions: how to exploit globally available soil moisture products to estimate antecedent soil wetness conditions in Morocco. – Natural Hazards and Earth System Sciences 20(10): 2591-2607. <https://doi.org/10.5194/nhess-20-2591-2020>.
- [41] Mahmoud, S. H., Gan, T. Y. (2018): Multi-criteria approach to develop flood susceptibility maps in arid regions of Middle East. – Journal of Cleaner Production 196: 216-229. <https://doi.org/10.1016/j.jclepro.2018.06.047>.
- [42] MoUD of GOI (2015): City Development Plan for Nagpur. – Ministry of Urban Development, Government of India, Capacity Building for Urban Development 2041(March).
- [43] Nachappa, T. G., Pirailiou, S. T., Ghorbanzadeh, O., Rahmati, O., Blaschke, T. (2020): Flood susceptibility mapping with machine learning, multi-criteria decision analysis and ensemble using Dempster Shafer theory. – Journal of Hydrology 125275. <https://doi.org/10.1016/j.jhydrol.2020.125275>.
- [44] Natarajan, L., Usha, T., Gowrappan, M., Palpanabhan Kasthuri, B., Moorthy, P., Chokkalingam, L. (2021): Flood susceptibility analysis in Chennai Corporation using frequency ratio model. – Journal of the Indian Society of Remote Sensing 49(7): 1533-1543. <https://doi.org/10.1007/s12524-021-01331-8>.
- [45] NEERI (2019): Environmental Status Report: Nagpur City 2019-20. – https://www.nmcnagpur.gov.in/assets/250/2021/06/mediafiles/Final_2020_ESR_-_AK.pdf.
- [46] Nkwunonwo, U. C., Whitworth, M., Baily, B. (2020): A review of the current status of flood modelling for urban flood risk management in the developing countries. – Scientific African 7: e00269. <https://doi.org/10.1016/j.sciaf.2020.e00269>.

- [47] Nohani, E., Moharrami, M., Sharafi, S., Khosravi, K., Pradhan, B., Pham, B. T., Lee, S., Melesse, A. M. (2019): Landslide susceptibility mapping using different GIS-Based bivariate models. – *Water (Switzerland)* 11(7): 0-22. <https://doi.org/10.3390/w11071402>.
- [48] NRSC National Remote Sensing Centre (2014): Land use/land cover database on 1:50,000 scale. – Natural Resources Census Project, LUCMD, LRUMG, RSAA, National Remote Sensing Centre, ISRO, Hyderabad. Technical Report Ver.1, 1-9. <https://bhuvan-app1.nrsc.gov.in/2dresources/thematic/2LULC/lulc1112.pdf>.
- [49] Nsangou, D., Kpoumié, A., Mfonka, Z., Ngouh, A. N., Fossi, D. H., Jourdan, C., Mbele, H. Z., Mouncherou, O. F., Vandervaere, J. P., Ndam Ngoupayou, J. R. (2022): Urban flood susceptibility modelling using AHP and GIS approach: case of the Mfoundi watershed at Yaoundé in the South-Cameroon plateau. – *Scientific African* 15: e01043. <https://doi.org/10.1016/j.sciaf.2021.e01043>.
- [50] Osti, R., Tanaka, S., Tokioka, T. (2008): Flood hazard mapping in developing countries: problems and prospects. – *Disaster Prevention and Management: An International Journal* 17(1): 104-113. <https://doi.org/10.1108/09653560810855919>.
- [51] Pal, B., Samanta, S. (2011): Surface runoff estimation and mapping using remote sensing and geographic information system. – *International Journal of Advances in Science and Technology* 3(3): 106-114.
- [52] Pham, B. T., Avand, M., Janizadeh, S., Phong, T. V., Al-Ansari, N., Ho, L. S., Das, S., Le, H. V., Amini, A., Bozchaloei, S. K., Jafari, F., Prakash, I. (2020): GIS based hybrid computational approaches for flash flood susceptibility assessment. – *Water (Switzerland)* 12(3). <https://doi.org/10.3390/w12030683>.
- [53] Pincetl, S., Franco, G., Grimm, N. B., Hogue, T. S., Hughes, S., Pardyjak, E., Kinoshita, A. M., Jantz, P., Gilchrist, M. (2013): Urban areas. Assessment of Climate Change in the Southwest United States: A Report Prepared for the National Climate Assessment. – https://doi.org/10.5822/978-1-61091-484-0_13.
- [54] Priya, V. (2019): Hydraulic Flood Modelling Using MIKE URBAN Software: An Application to Chennai City. – Conference: Hydro 2012, Chennai, March 2019.
- [55] Rahman, M., Ningsheng, C., Islam, M. M., Dewan, A., Iqbal, J., Washakh, R. M. A., Shufeng, T. (2019): Flood susceptibility assessment in Bangladesh using machine learning and multi-criteria decision analysis. – *Earth Systems and Environment* 3(3): 585-601. <https://doi.org/10.1007/s41748-019-00123-y>.
- [56] Rahman, M., Ningsheng, C., Mahmud, G. I., Islam, M. M., Pourghasemi, H. R., Ahmad, H., Habumugisha, J. M., Washakh, R. M. A., Alam, M., Liu, E., Han, Z., Ni, H., Shufeng, T., Dewan, A. (2021): Flooding and its relationship with land cover change, population growth, and road density. – *Geoscience Frontiers* 12(6): 101224. <https://doi.org/10.1016/j.gsf.2021.101224>.
- [57] Rahmati, O., Pourghasemi, H. R., Zeinivand, H. (2016): Flood susceptibility mapping using frequency ratio and weights-of-evidence models in the Golastan Province, Iran. – *Geocarto International* 31(1): 42-70. <https://doi.org/10.1080/10106049.2015.1041559>.
- [58] Rai, P. K., Chahar, B. R., Dhanya, C. T. (2017): GIS-based SWMM model for simulating the catchment response to flood events. – *Hydrology Research* 48(2): 384-394. <https://doi.org/10.2166/nh.2016.260>.
- [59] Regmi, A. D., Yoshida, K., Pourghasemi, H. R., Dhital, M. R., Pradhan, B. (2014): Landslide susceptibility mapping along Bhalubang–Shiwapur area of mid-Western Nepal using frequency ratio and conditional probability models. – *Journal of Mountain Science*. <https://doi.org/10.1007/s11629-013-2847-6>.
- [60] Rezaie, F., Bateni, S. M., Heggy, E., Lee, S. (2021): Utilizing the SAR, GIS, and Novel Hybrid Metaheuristic-GMDH Algorithm for Flood Susceptibility Mapping. – *IEEE*. <https://doi.org/10.1109/IGARSS47720.2021.9553468>.
- [61] Rincón, D., Khan, U. T., Armenakis, C. (2018): Flood risk mapping using GIS and multi-criteria analysis: a greater Toronto area case study. – *Geosciences (Switzerland)* 8(8). <https://doi.org/10.3390/geosciences8080275>.

- [62] Samanta, S., Pal, D. K., Palsamanta, B. (2018): Flood susceptibility analysis through remote sensing, GIS and frequency ratio model. – *Applied Water Science* 8(2): 1-14. <https://doi.org/10.1007/s13201-018-0710-1>.
- [63] Shafizadeh-Moghadam, H., Valavi, R., Shahabi, H., Chapi, K., Shirzadi, A. (2018): Novel forecasting approaches using combination of machine learning and statistical models for flood susceptibility mapping. – *Journal of Environmental Management* 217: 1-11. <https://doi.org/10.1016/j.jenvman.2018.03.089>.
- [64] Sörensen, J., Persson, A., Sternudd, C., Aspegren, H., Nilsson, J., Nordström, J., Jönsson, K., Mottaghi, M., Becker, P., Pilesjö, P., Larsson, R., Berndtsson, R., Mobini, S. (2016): Re-thinking urban flood management—time for a regime shift. – *Water* 8(8): 332. <https://doi.org/10.3390/w8080332>.
- [65] Steiner, J., Grillmair, E. (1973): Possible galactic causes for periodic and episodic glaciations. – *Geological Society of America Bulletin* 84 (3): 1003-1018. [https://doi.org/10.1130/0016-7606\(1973\)84<1003:PGCFPA>2.0.CO;2](https://doi.org/10.1130/0016-7606(1973)84<1003:PGCFPA>2.0.CO;2).
- [66] Swain, K. C., Singha, C., Nayak, L. (2020): Flood susceptibility mapping through the GIS-AHP technique using the cloud. – *ISPRS International Journal of Geo-Information* 9(12). <https://doi.org/10.3390/ijgi9120720>.
- [67] Symeonakis, E., Drake, N. (2010): 10-Daily soil erosion modelling over sub-Saharan Africa. – *Environmental Monitoring and Assessment* 161(1-4): 369-387. <https://doi.org/10.1007/s10661-009-0754-7>.
- [68] Tang, Z., Yi, S., Wang, C., Xiao, Y. (2018): Incorporating probabilistic approach into local multi-criteria decision analysis for flood susceptibility assessment. – *Stochastic Environmental Research and Risk Assessment* 32(3): 701-714. <https://doi.org/10.1007/s00477-017-1431-y>.
- [69] Tehrany, M. S., Lee, M. J., Pradhan, B., Jebur, M. N., Lee, S. (2014): Flood susceptibility mapping using integrated bivariate and multivariate statistical models. – *Environmental Earth Sciences* 72(10): 4001-4015. <https://doi.org/10.1007/s12665-014-3289-3>.
- [70] Termeh, S. V. R., Kornejady, A., Pourghasemi, H. R., Keesstra, S. (2018): Flood susceptibility mapping using novel ensembles of adaptive neuro fuzzy inference system and metaheuristic algorithms. – *Science of the Total Environment* 615: 438-451. <https://doi.org/10.1016/j.scitotenv.2017.09.262>.
- [71] Tingsanchali, T. (2012): Urban flood disaster management. – *Procedia Engineering* 32: 25-37. <https://doi.org/10.1016/j.proeng.2012.01.1233>.
- [72] Tucci, C. E. C. (2001): Urban drainage issues in developing countries. – *Urban Drainage in Humid Tropics* 40: 23-40.
- [73] Vasconcelos, A. F., Barbassa, A. P. (2021): Sustainable urban stormwater management in developing countries: integrating strategies to overcome Brazilian barriers. – *Urban Water Journal*. <https://doi.org/10.1080/1573062X.2021.1969415>.
- [74] Vilasan, R. T., Kapse, V. S. (2022a). Evaluation of the prediction capability of AHP and F-AHP methods in flood susceptibility mapping of Ernakulam district (India). – *Natural Hazards* 112: 1767-1793. <https://doi.org/10.1007/s11069-022-05248-4>.
- [75] Vilasan, R. T., Kapse, V. S. (2022b). Monitoring spatio-temporal dynamics of land use/land cover changes using remote sensing and GIS - A case study of Ernakulam District, India. – *Applied Ecology and Environmental Research* 20(July): 3353-3366. <https://doi.org/10.15666/aeer/2004>.
- [76] Vojtek, M., Vojteková, J. (2019): Flood susceptibility mapping on a national scale in Slovakia using the analytical hierarchy process. – *Water (Switzerland)* 11(2). <https://doi.org/10.3390/w11020364>.
- [77] Wang, Y., Hong, H., Chen, W., Li, S., Pamučar, D., Gigović, L., Drobnjak, S., Bui, D. T., Duan, H. (2019): A hybrid GIS multi-criteria decision-making method for flood susceptibility mapping at Shangyou, China. – *Remote Sensing* 11(1). <https://doi.org/10.3390/rs11010062>.

- [78] Waqas, H., Lu, L., Tariq, A., Li, Q., Baqa, M. F., Xing, J., Sajjad, A. (2021): Flash flood susceptibility assessment and zonation using an integrating analytic hierarchy process and frequency ratio model for the Chitral District, Khyber Pakhtunkhwa, Pakistan. – *Water (Switzerland)* 13(12). <https://doi.org/10.3390/w13121650>.
- [79] Webster, P., West, J. R., Gurnell, A. M., Sadler, J. P. (2001): Development, flood risk and the urban environment: experiences from the River Tame. – *Water and Environment Journal* 15(3): 167-173. <https://doi.org/doi:10.1111/j.1747-6593.2001.tb00328.x>.
- [80] Wedajo, G. K. (2017): LiDAR DEM data for flood mapping and assessment; opportunities and challenges: a review. – *Journal of Remote Sensing & GIS* 06(04): 2015-2018. <https://doi.org/10.4172/2469-4134.1000211>.
- [81] Yariyan, P., Avand, M., Abbaspour, R. A., Torabi Haghighi, A., Costache, R., Ghorbanzadeh, O., Janizadeh, S., Blaschke, T. (2020): Flood susceptibility mapping using an improved analytic network process with statistical models. – *Geomatics, Natural Hazards and Risk* 11(1): 2282-2314. <https://doi.org/10.1080/19475705.2020.1836036>.